THE FASEB JOURNAL • RESEARCH • www.fasebj.org

The regulation of proteostasis in glial cells by nucleotide receptors is key in acute neuroinflammation

Laura de Diego García,[*,†] Álvaro Sebastián-Serrano,[*,†,1,2] Ivó H. Hernández,[‡,§,¶] Jesús Pintor,[‖] José J. Lucas,[‡,¶] and Miguel Díaz-Hernández[*,†,3]

[*]Department of Biochemistry and Molecular Biology, and [‖]Faculty of Optic and Optometry, Universidad Complutense of Madrid, Madrid, Spain; [†]Instituto de Investigación Sanitaria del Hospital Clínico San Carlos (IdISSC), Madrid, Spain; [‡]Centro de Biología Molecular Severo Ochoa, Consejo Superior de Investigaciones Científicas–Universidad Autónoma de Madrid (CSIC–UAM), Madrid, Spain; [§]Departamento de Biología, Facultad de Ciencias, UAM, Madrid, Spain; and [¶]Networking Research Center on Neurodegenerative Diseases (CIBERNED), Instituto de Salud Carlos III, Madrid, Spain

ABSTRACT: The disturbances of cellular proteostasis caused by the alteration in the ubiquitin-proteasome system (UPS) have been proposed as a common mechanism underlying several neural pathologies that involve a neuroinflammatory process. As we have previously reported that the nucleotide receptor P2Y purinoceptor 2 ($P2Y_2R$) regulates the proteasomal catalytic activities, we wonder whether this receptor is involved in the UPS disturbances associated with the neuroinflammation process. With the use of mice expressing a UPS reporter [mice expressing the UPS reporter ubiquitin^{G76V}-green fluorescent protein (UbGFP mice)], we found that LPS-induced acute neuroinflammation status causes a UPS impairment in astrocytes and microglial cells by a mechanism dependent on $P2Y_2R$. In this line, LPS-treated double transgenic mice expressing a UPS reporter and $P2Y_2R$-deficient mice did not present a UPS impairment in astrocytes or a social interaction deficit as severe as that observed in LPS-treated UbGFP mice. *In vivo* administration of selective $P2Y_2R$ agonist diuridine tetraphosphate reversed the UPS impairment completely in astrocytes and partially in microglial cells, promoting increased expression of the proteasomal β5 subunit by a mechanism dependent on the nonreceptor tyrosine kinases family/PI3K/ERK pathway. Altogether, our results suggest that LPS induces unbalanced proteostasis in astrocytes by blocking $P2Y_2R$. Finally, our findings point to the design of selective $P2Y_2R$ agonist drugs as a new therapeutic approach to treat the neuroinflammatory status.—De Diego-García, L., Sebastián-Serrano, Á., Hernández, I. H., Pintor, J., Lucas, J. J., Díaz-Hernández, M. The regulation of proteostasis in glial cells by nucleotide receptors is key in acute neuroinflammation. FASEB J. 32, 000–000 (2018). www.fasebj.org

KEY WORDS: $P2Y_2R$ · Up_4U · LPS · astrocytes · ubiquitin-proteasome system

Cellular proteostasis encompasses the intracellular biologic pathways that control the biogenesis, folding, trafficking, and degradation of proteins. Perturbation of neural cell proteostasis has been associated with different pathologic processes, including neurodegenerative diseases or inflammatory disorders, although the underlying mechanisms are still not sufficiently understood (1–3). The ubiquitin-proteasome system (UPS) contributes to the cellular proteostasis, degrading intracellular proteins. After the covalent attachment of multiple ubiquitin molecules, the target proteins are degraded by the 26S proteasome complex (4–6). The 26S proteasome complex is composed of 2 subcomplexes: a 20S core particle, where proteolysis takes place, and a 19S regulatory particle that prepares substrates to enter into the 20S. The 20S complex consists of 4 heptameric rings composed by 2 types of subunits: α and β subunits. The β1, β2, and β5 subunits are associated with postglutamyl (PG-L)-, trypsin-, and chymotrypsin (CT-L)-like catalytic activities, respectively (7). The 26S proteasome complex is continually assembled and

ABBREVIATIONS: CT-L, chymotrypsin-like; DG, dentate gyrus; GAPDH, glyceraldehyde-3-phosphate dehydrogenase; GCDG, green cells in the dentate gyrus; GFAP, glial fibrillary acidic protein; GFP, green fluorescent protein; Iba-1, ionized calcium-binding adapter molecule 1, microglial antigen; NeuN, neuronal nuclei antigen; $P2Y_2$, P2Y purinoceptor 2; $P2Y_2R$, nucleotide receptor P2Y purinoceptor 2; $P2Y_2R^{-/-}$, nucleotide receptor P2Y purinoceptor 2 deficient; PG-L, postglutamyl-like; Src, nonreceptor tyrosine kinases family; Ub^{G76V}-GFP, ubiquitin^{G76V}-green fluorescent protein; UbGFP mice, mice expressing the ubiquitin-proteasome system reporter ubiquitin^{G76V}-green fluorescent protein; UbGFP, $P2Y_2R^{-/-}$ mice, double transgenic mice expressing a ubiquitin-proteasome system reporter and nucleotide receptor P2Y purinoceptor 2 deficient; Up_4U, diuridine tetraphosphate; UPS, ubiquitin-proteasome system; WT, wild type

[1] Current affiliation: Instituto de Investigaciones Biomédicas "Alberto Sols," Consejo Superior de Investigaciones Científicas–Universidad Autónoma de Madrid (CSIC–UAM), Madrid, Spain.

[2] Current affiliation: Centro de Investigación Biomédica en Red sobre Enfermedades Neurodegenerativas (CIBERNED), Instituto de Salud Carlos III, Madrid, Spain.

[3] Correspondence: Department of Biochemistry and Molecular Biology, Veterinary School, Universidad Complutense of Madrid, Avda. Puerta de Hierro S/N, 28040 Madrid, Spain. E-mail: migueldiaz@ucm.es

doi: 10.1096/fj.201701064RR

This article includes supplemental data. Please visit *http://www.fasebj.org* to obtain this information.

disassembled, and mature proteasome is also directly modified in response to environmental factors (8). Indeed, the neuroinflammation induced by LPS has been related to alterations in the expression of the 20S catalytic subunits β5 and β5i, as well as in the catalytic proteasomal activity (9–11). Additionally, the proteasome 20S complex subunit β4 and the 19S complex subunit Rpn9 have been, respectively, involved in the neuronal loss (12) and the production of proinflammatory mediators (13) caused by LPS-induced neuroinflammation. However, which molecular mechanisms underlying the proteasomal alterations are produced by the LPS-induced neuroinflammation, as well as which neural lineages are more susceptible to these changes, are still unresolved questions.

Under pathologic conditions, such as neuroinflammation, together with other proinflammatory molecules, nucleotides are also released from brain parenchyma (14). These compounds act as extracellular signaling molecules in the CNS, activating specific receptors—denominated P2 receptors—on the surface of the different lineages that shape the brain tissue (14). In both cellular and animal models of LPS-induced neuroinflammation, it has been found that the metabotropic P2Y purinoceptor 2 receptor ($P2Y_2R$) was upregulated (15–18) and suggested that this receptor might play a key role in the cellular response to neuroinflammation (19). With support for this hypothesis, under LPS-induced neuroinflammation, $P2Y_2R$ activation potentiates the transendothelial migration of neutrophils (20), promotes the secretion of proinflammatory factors from macrophages (18), and regulates the migration and phagocytic ability of microglia (21). However, other groups have found that activation of $P2Y_2R$ attenuates the microglial activation (22) and protects associations to LPS-induced neuroinflammation from neuronal death (23).

In a recent work, we reported, for the first time, that $P2Y_2R$ modulates the UPS activity in hippocampal cells by regulating the expression of catalytic proteasome subunits β1 and β5 (24). In the current study, we decided to explore whether $P2Y_2R$ is involved in the changes suffered by the proteasome of hippocampal neural cells in a neuroinflammatory environment. To address this question, we induced an acute neuroinflammatory state by intraperitoneal administration of LPS, both in UPS reporter mice (25) and in the double transgenic mice crossbreeding the UPS reporter mice and mice deficient in $P2Y_2R$ [UPS reporter ubiquitin^{G76V}-green fluorescent protein (Ub^{G76V}-GFP; UbGFP; P2Y2R$^{-/-}$)] (26). With the use of this experimental approach, we found that $P2Y_2R$ is essential to change the proteasome conformation in glial cells under an LPS-induced acute neuroinflammation. In addition, we found that *in vivo* activation of $P2Y_2R$ prevents the decrease of UPS activity in astrocytes associated to neuroinflammation.

MATERIALS AND METHODS

Animals

All animal procedures were carried out at the Universidad Complutense of Madrid, in compliance with national and European regulations (RD1201/2005; 86/609/CEE), following the guidelines of the International Council for Laboratory Animal Science. All animals were housed with food and water available *ad libitum* and maintained in a temperature-controlled environment on a 12/12 h light/dark cycle with light onset at 8 AM.

$P2Y_2R^{-/-}$ mice (26) were provided by The Jackson Laboratory, (Bar Harbor, ME, USA), and mice expressing UbGFP (25) were provided by Dr. J. J. Lucas (CBMSO, Madrid, Spain).

Cell culture, transfection, and treatment conditions

Primary astrocytes and microglia cultures were prepared from the hippocampus of wild-type (WT) or $P2Y_2R^{-/-}$ mice at postnatal 4–5 d. The cultures were maintained in a 37°C incubator with a humidified atmosphere of 5% CO_2. The medium was replaced every 3 d, and cells were maintained for 12–14 d in culture until reaching confluence. To separate astrocytes and microglia, the flasks were shaken at 250 rpm for 2 h at 37°C in an orbital shaker, and after that, the supernatant containing microglia and astrocytes was adhered to the culture surface. The astrocyte adherent monolayer was detached with trypsin 0.05% and 0.2 mM EDTA. Then, astrocytes and microglia cells were plated at 7×10^5 cells/well in 6-well plates and cultured in supplemented DMEM media (Thermo Fisher Scientific, Waltham, MA, USA).

Human glioblastoma astrocytoma cell line U87 was plated at 7.5 × 105 cells/well in 6-well plates and cultured in supplemented DMEM media (Thermo Fisher Scientific). For the experiments where a transfection was required, cells were transiently transfected using Lipofectamine 2000 (Thermo Fisher Scientific), 24 h after being plated. The plasmids encoding Ub^{G76V}-GFP and ubiquitin-M-yellow fluorescent protein were provided by J.J.L. and Addgene (Cambridge, MA, USA), respectively.

Forty-eight hours after plating, cells were stimulated with different drugs for the indicated periods. The selective inhibitors for the different kinases and the proteasome inhibitors assayed were preincubated for 20 min before the addition of the selective $P2Y_2R$ agonist, diuridine tetraphosphate (Up_4U).

Chemical and antibodies

LPS, lactacystin, epoxomicin, and the antibodies anti-glyceraldehyde-3-phosphate dehydrogenase (GAPDH), anti-β-actin, and anti-α-tubulin were purchased from MilliporeSigma (Madrid, Spain); LY294002 and suramin were supplied from Tocris Bioscience (Bristol, United Kingdom). Z-Ile-Glu(OtBu)-Ala-Leu-CHO (PSI), 4-amino-3-(4-chlorophenyl)-1-(*t*-butyl)-1H-pyrazolo[3,4-d]pyrimidine, 4-amino-5-(4-chlorophenyl)-7-(*t*-butyl)pyrazolo[3,4-d]pyrimidine (PP-2), and anti-neuronal nuclei antigen (NeuN) antibody were obtained from Merck Millipore (Tullagreen, Ireland). Dinucleotide Up_4U (INS365) was provided from Inspire Pharmaceuticals (Raleigh, NC, USA). The commercial antibody for $P2Y_2R$ was purchased from Alomone Labs (Jerusalem, Israel). Antibodies against β1, β2, β5, β1i, β2i, and β5i were obtained from Enzo Life Science (Farmingdale, NY, USA). Antibodies against GFP were obtained from Thermo Fisher Scientific and AvesLab (Tigard, OR, USA). Antibody against glial fibrillary acidic protein (GFAP) was supplied by Santa Cruz Biotechnology (Dallas, TX, USA). Antibody against ionized calcium-binding adapter molecule 1 (Iba-1) was provided by Wako (Richmond, VA, USA).

Stereotaxic injection

Six-month-old mice were anesthetized with isoflurane (1-chloro-2,2,2-trifluoroethyl-difluormethylether; Isovet; Braun, Rubi, Barcelona, Spain), diluted in 50% O_2. The scalp was incised along the midline, and 1 hole was made at the appropriate stereotaxic coordinates from bregma (mediolateral, 1 mm; anteroposterior,

0.5 mm; dorsoventral, 2.5 mm). Intracerebroventricular administration of 2 μl of 45 mM Up_4U, 2 μl of PBS, or 2 μl of 1.5 mM suramin was infused at a rate of ≈1 μl/min.

RT-PCR and quantitative real-time PCR

RNA isolation (from hippocampal tissue of UbGFP mice, cultured microglia or astrocytes) and RT reactions were performed as previously described (24). PCRs were carried out using AmpliTaq Gold Master Mix (Applied Biosystems, Madrid, Spain), 5 μl of the RT product, and specific commercial oligonucleotide primers for $P2Y_2R$ (Mm02619978_s1 from Applied Biosystems) or for Ub^{G76V}-GFP (24) and GAPDH (Applied Biosystems). Amplified PCR products were electrophoresed on a 1% agarose gel and visualized by SYBR Safe DNA gel stain.

Real-time quantitative PCRs were carried out using LuminoCt qPCR Readymix (MilliporeSigma), 5 μl of the RT product, and gene-specific primers and TaqMan minor groove binder probes for $P2Y_2R$, Ub^{G76V}-GFP, and GAPDH (Mm02619978_s1 and Mm99999915_g1; Applied Biosystems). Fast thermal cycling was performed using a StepOnePlus Real-Time PCR System (Applied Biosystems). The results were normalized, as indicated by the parallel amplification of the endogenous control GAPDH.

Western blotting

Cultured microglia or astrocytes cells, U87 cells, and hippocampal samples from WT, UbGFP, $P2Y_2R^{-/-}$, or UbGFP; $P2Y_2R^{-/-}$ mice were treated with lysis buffer containing 20 mM 4-(2-hydroxyethyl)-1-piperazineethanesulfonic acid, 100 mM NaCl, 50 mM NaF, 5 mM EDTA, 5 mM Na_3VO_4 (all salts from MilliporeSigma), 1% Triton X-100, okadaic acid, and Complete Protease Inhibitor Cocktail Tablets, pH 7.4 (Roche Diagnostics GmbH, Berlin, Germany). Protein concentration was determined, and then, samples were boiled in gel-loading buffer and separated by SDS-PAGE. Proteins were transferred to nitrocellulose membranes and probed with the following primary antibodies: rabbit anti- $P2Y_2R$ (1:200), rabbit anti-GFP (1:1000), mouse anti-β1 (1:1000), mouse anti-β2 (1:1000), rabbit anti-β5 (1:1000), mouse anti-β1i (1:1000), rabbit anti-β2i (1:1000), mouse anti-β5i (1:1000), mouse anti-α-tubulin (1:10,000), mouse anti-GAPDH (1:10,000), and mouse anti β-actin (1:10,000). Blots were then washed in PBS-Tween and incubated with goat anti-rabbit or goat anti-mouse IgGs, coupled with horseradish peroxidase (Amersham GE Healthcare, Amersham, United Kingdom), used at 1:1000 and 1:5000, respectively. Protein bands were visualized by chemiluminescence (Pierce Biotechnology, Rockford, IL, USA) using ImageQuant LAS500 (GE Healthcare Life Sciences) and analyzed using ImageJ software (v.1, 47d; National Institutes of Health, Bethesda, MD, USA).

Proteasome activity assays

To determine proteasome activity, we followed the procedure previously described (27). In brief, samples from cultured astrocytes or microglia from WT or $P2Y_2R^{-/-}$ mice or U87 cells were adjusted to 0.5 mg/ml total protein by dilution with extraction buffer. CT-L and PG-L activities were determined using 100 μM Suc-Leu-Leu-Val-Tyr-aminomethylcoumarin and 200 μM Z-Leu-Leu-Glu-β-2-naphthylamine, respectively. Background activity was determined by addition of the proteasome inhibitor MG132 at a final concentration of 10 μM. All reagents were from MilliporeSigma.

Behavior experiments: social exploratory test

Six-month-old WT and $P2Y_2R^{-/-}$ female mice, weighing 25–30 g, were randomly divided within each cage and handled 2 min each day for 7 d before experimentation to accustom them to routine handling. For all experiments, young adult mice were intraperitoneally treated with either sterile PBS or LPS (5 mg/kg, *Escherichia coli*, serotype 055: B5; MilliporeSigma), 10 min before behavioral testing. To assess the motivation to engage in social exploratory behavior (28, 29), a novel, female juvenile mouse was introduced into the test subject's home cage for a 10-min period. Behavior was videotaped, and the cumulative amount of time that the subject engaged in the social investigation was determined from the video records by a trained observer who was blind to the experimental treatments. Social behavior was determined as the amount of time that the experimental subject spent investigating (*e.g.*, anogenital sniffing, trailing) the juvenile. Results are expressed as the percent decrease in time engaged in social behavior compared with respective baseline measures.

Immunofluorescence studies

For confocal microscopy, animals were transcardially perfused with 4% paraformaldehyde in Sorensen's buffer for 10 min, postfixed, and cryoprotected in sucrose before sectioning. Tissue slices were washed in PBS and treated with blocking solution containing 5% fetal bovine serum, 1% bovine serum albumin, and 0.2% Triton-X 100 in PBS buffer. After that, samples were incubated with primary antibodies, diluted in blocking solution. After washing them, sections were incubated with fluorescent-tagged secondary antibodies to be counterstained with DAPI dihydrochloride (Thermo Fisher Scientific) and mounted in FluorSave (Merck Millipore) later. The following primary antibodies were used at the indicated dilutions: rabbit anti-GFP 1:400, chicken anti-GFP 1:400, rabbit anti-$P2Y_2R$ 1:200, mouse anti-NeuN 1:100, mouse anti-GFAP 1:200, and rabbit anti-Iba-1 1:300. Donkey anti-rabbit, -mouse, or -chicken secondary antibodies, conjugated with Alexa 488, 594, or 647 (Thermo Fisher Scientific), were used at 1:500. Confocal images were acquired with a true point-scanning, spectral system for fluorescence imaging (TCS SPE) confocal microscope, equipped with 4 laser lines (405, 488, 561, and 653 nm), using a ×20 or 40 dry objective (Leica Microsystems, Wetzlar, Germany) and using Leica software Leica Application Suite Advance Fluorescence (LAS AF) v.2.2.1 (Leica Microsystems). Green cells in dentate gyrus (GCDG) were considered those cells positively marked with antibodies against GFP, with an identifiable cellular morphology, and whose nucleus was positively stained with DAPI.

Statistical analysis

Results were analyzed by unpaired Student's *t* test or ANOVA test, followed by Bonferroni's or Sidak's multiple comparison tests, using GraphPad Prism 6 (GraphPad Software, La Jolla, CA, USA), and expressed as the means ± SEM. Differences were considered to be significant at $P < 0.05$.

RESULTS

Acute neuroinflammation alters the functionality of UPS in glial cells from hippocampal dentate gyrus

Initially, we investigated whether the induction of an acute neuroinflammatory state can alter the functionality of UPS in hippocampal dentate gyrus (DG) cells. To monitor the UPS activity, we used the transgenic UbGFP mice. These mice ubiquitously express the ubiquitin fusion degradation substrate Ub^{G76V}-GFP (25). This reporter protein will

accumulate in those cells where there is an impaired UPS. An acute neuroinflammatory state was induced in adult UbGFP mice by a single intraperitoneal injection of LPS at 5 mg/kg of body weight. Control animals were injected intraperitoneally with the same volume of vehicle solution (PBS). Forty-eight hours after injection, animals were euthanized and their brains processed to analyze the hippocampal DG by immunofluorescence techniques (**Fig. 1*A***). Additional groups of UbGFP mice were intracerebroventricularly treated for 48 h with 2 μl lactacystin (10 μg/μl), a selective proteasome inhibitor, or with the same volume of PBS. The initial analysis revealed that PBS-treated UbGFP mice *via* intraperitoneal injection showed a similar number of GCDG than those PBS treated intracerebroventricularly (Fig. 1*A, B*). As expected, lactacystin administration tripled the number of cells that accumulated the Ub^{G76V}-GFP reporter in DG, in contrast to those detected in PBS-treated mice (intracerebroventricularly; lactacystin 35.0 ± 3.8 GCDG per 0.1 mm^3 *vs.* PBS 11.2 ± 1.0 GCDG per 0.1 mm^3; Fig. 1*A, B*). In a similar way, LPS-treated UbGFP mice (intraperitoneally) showed more than double GCDG than PBS-treated UbGFP mice (intraperitoneally; LPS 25.4 ± 2.4 GCDG per 0.1 mm^3; Fig. 1*A, B*). It is to highlight that the increased Ub^{G76V}-GFP protein expression detected in LPS-treated UbGFP mice did not correlate with alterations at a transcriptional (Fig. 1*C*) or translational (Supplemental Fig. 1*A, B*) level. In addition, double immunolabeling, using astrocyte (GFAP)-, microglia (Iba-1)-, or neuron (NeuN)-specific markers (Fig. 1*D*), revealed that the increased accumulation of the Ub^{G76V}-GFP reporter took place mainly in glial cells. More precisely, whereas only a few GFP-positive cells were identified as microglial (0.1 ± 0.1 GCDG/0.1 mm^3 positively marked with antibody anti-Iba-1) or as astrocytes (1.1 ± 0.2 GCDG/0.1 mm^3 positively marked with antibody anti-GFAP) in PBS-treated mice (intraperitoneally), the number of both cellular types significantly increased in LPS-treated UbGFP mice (intraperitoneally; microglia 9.3 ± 2.2 GCDG/0.1 mm^3 and astrocytes 6.9 ± 1.2 GCDG/0.1 mm^3; Fig. 1*E*). Regarding the neuronal lineage, the number of GCDG labeled with the neuronal marker NeuN was similar in PBS- and LPS-treated mice (intraperitoneally; 9.0 ± 1.0 and 6.3 ± 1.4 of GCDG/0.1 mm^3, respectively; Fig. 1*E*). With the support that the neuroinflammatory environment influences the proteasomal functionality, a significant reduction in constitutive, catalytic, proteasomal β5 subunits, linked to a significant increase of inducible, catalytic, proteasomal β5i subunits, was observed in LPS-treated mice (Fig. 1*F*). However, no changes in the others constitutive or inducible catalytic proteasomal subunits were observed (Fig. 1*F*). All of these results suggest that an acute neuroinflammation alters the UPS functionality both in hippocampal astrocytes and microglial cells.

Acute neuroinflammation increases expression of $P2Y_2R$ in glial cells

In agreement with previous studies, where it was reported that LPS-induced neuroinflammation upregulates the $P2Y_2R$ expression (30), a significant increase in protein levels of this receptor was detected in the hippocampus of LPS-treated UbGFP mice (intraperitoneally; **Fig. 2*A***). Additional analysis, using specific glial markers, revealed that LPS treatment did not alter either the number of astrocytes expressing $P2Y_2R$ nor the total number of astrocytes, with respect to those detected in PBS-treated mice (intraperitoneally; Fig. 2*B–D*). However, in the case of microglial cells, despite that LPS did not modify their total number, a significant increase in those expressing $P2Y_2R$ was detected in LPS-treated mice (intraperitoneally; Fig. 2*B–D*).

As astrocytes and microglial cells were the lineages most sensitive to altering their UPS by the endotoxin, we decided to evaluate whether LPS induces an upregulation of $P2Y_2R$, specifically in these cells. To address this question, we used primary cultures of astrocytes and microglia cells from mouse hippocampus. These studies confirmed that astrocytes treated with 0.3 μg/ml LPS for 48 h significantly increased the messenger and protein levels of $P2Y_2R$ compared with those detected when these were treated with PBS (Fig. 2*E, F*). However, in microglial cells, a significant increase of the messenger, but not the protein levels of $P2Y_2R$, was detected (Fig. 2*E, F*).

The $P2Y_2R$ is involved in the alteration of UPS functionality in glial cells caused by the LPS-induced acute neuroinflammation

In a next step, to elucidate whether $P2Y_2R$ plays a relevant role in the UPS alteration in glial cells under a neuroinflammation environment, we decided to crossbreed UbGFP animals with $P2Y_2R^{-/-}$ mice. At 6 mo old, UbGFP; $P2Y_2R^{-/-}$ mice were intraperitoneally treated with LPS or PBS for 48 h before being analyzed. It is worth noting that the initial analysis of UbGFP; $P2Y_2R^{-/-}$ revealed that these mice showed a slight increase in the total number of GCDG compared with that observed in UbGFP mice. Surprisingly, LPS-treated UbGFP; $P2Y_2R^{-/-}$ mice did not show the increase in the number of GCDG detected in UbGFP mice (PBS 16.9 ± 1.4 GCDG/0.1 mm^3 *vs.* LPS 13.8 ± 1.4 GCDG/0.1 mm^3; **Figs.** 1*A, B* and **3*A, B***). Cellular linage distribution analysis of GCDG in UbGFP; $P2Y_2R^{-/-}$ mice revealed that in a similar way to UbGFP mice, most of the GCDG belonged to the neuronal lineage in PBS-treated mice. Nevertheless, when these mice were LPS treated, the GCDG were identified as neurons and a reduced number of microglia cells but interestingly, none as astrocytes (Fig. 3*C*), suggesting that $P2Y_2R$ plays a key role in LPS-induced proteolysis alteration in astrocytes. It is also noteworthy that in UbGFP; $P2Y2R^{-/-}$ mice, the LPS treatment did not modify the levels of any constitutive or inducible catalytic proteasomal subunit (Fig. 3*D*).

The LPS-induced neuroinflammation causes behavioral alterations, such as anorexia, weight loss, as well as decreased social interactions (28, 29). To confirm that $P2Y_2R$ plays a relevant role in the LPS-induced neuroinflammatory process, we decided to subject the UbGFP mice and UbGFP; $P2Y_2R^{-/-}$ mice treated with LPS or vehicle to a social behavioral interaction test (**Fig. 4*A***). Our results revealed that both UbGFP and UbGFP; $P2Y_2R^{-/-}$ mice treated with PBS did not show any significant variations in their body weight or in the basal social

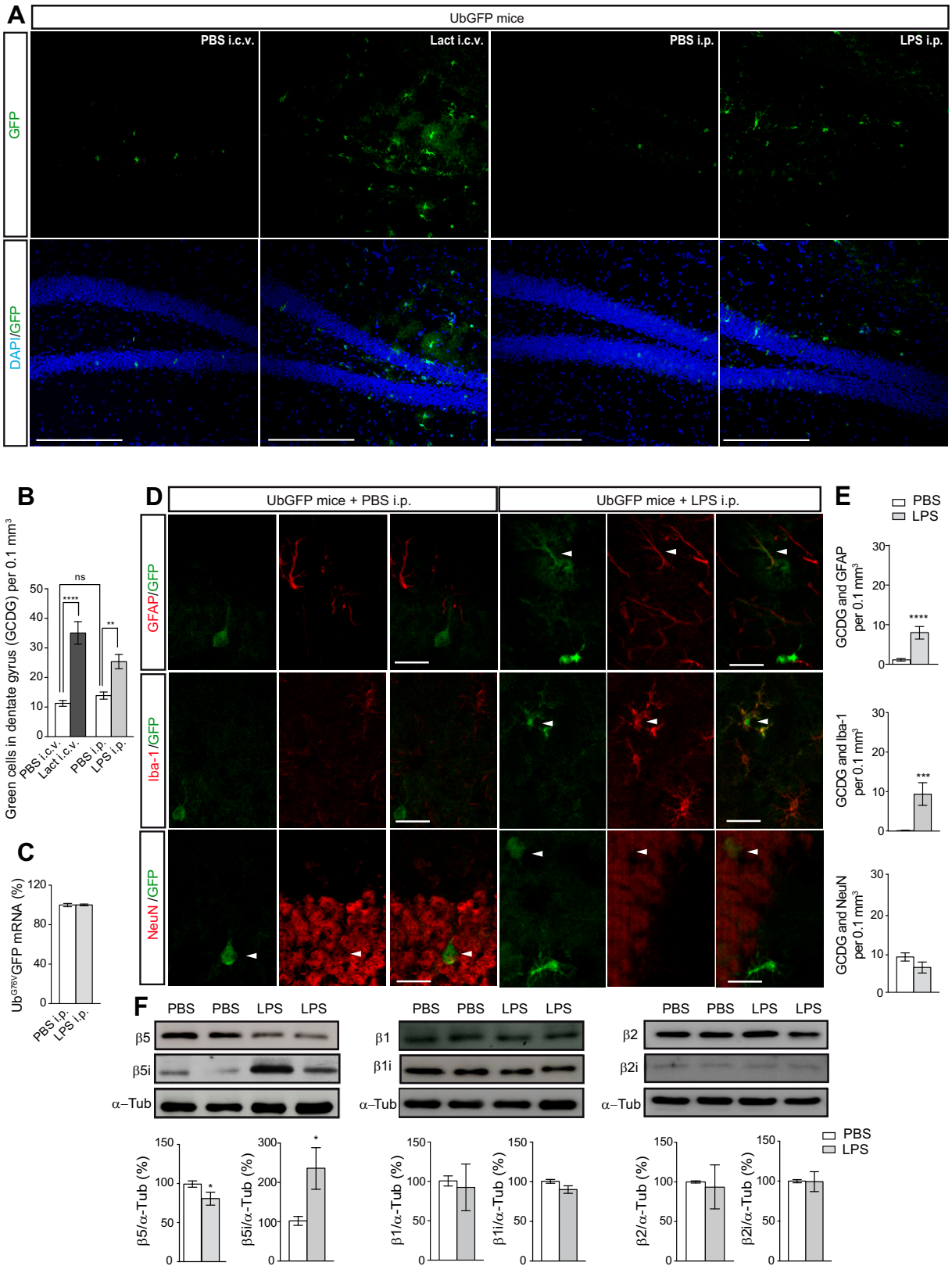

Figure 1. LPS-induced acute neuroinflammation impairs the UPS in hippocampal glial cells. *A*) Representative images of hippocampal coronal sections from UbGFP mice treated with PBS or LPS [intraperitoneally (i.p.)] or with PBS or lactacystin (Lact; intracerebroventricularly) and stained with antibody against GFP alone (upper) or with nuclear marker DAPI (lower). Original scale bars, 200 μm. *B*) Quantification of GCDG/0.1 mm^3 hippocampal DG ($n \geq 9$ mice/treatment; sections ≥5/mouse). Ns, nonsignificant using unpaired Student's *t* test. *C*) Analysis of Ub^{G76V}-GFP mRNA levels by quantitative RT-PCR in hippocampal samples from intraperitoneal PBS- or LPS-treated UbGFP mice ($n = 4$/treatment). One hundred percent value

(*continued on next page*)

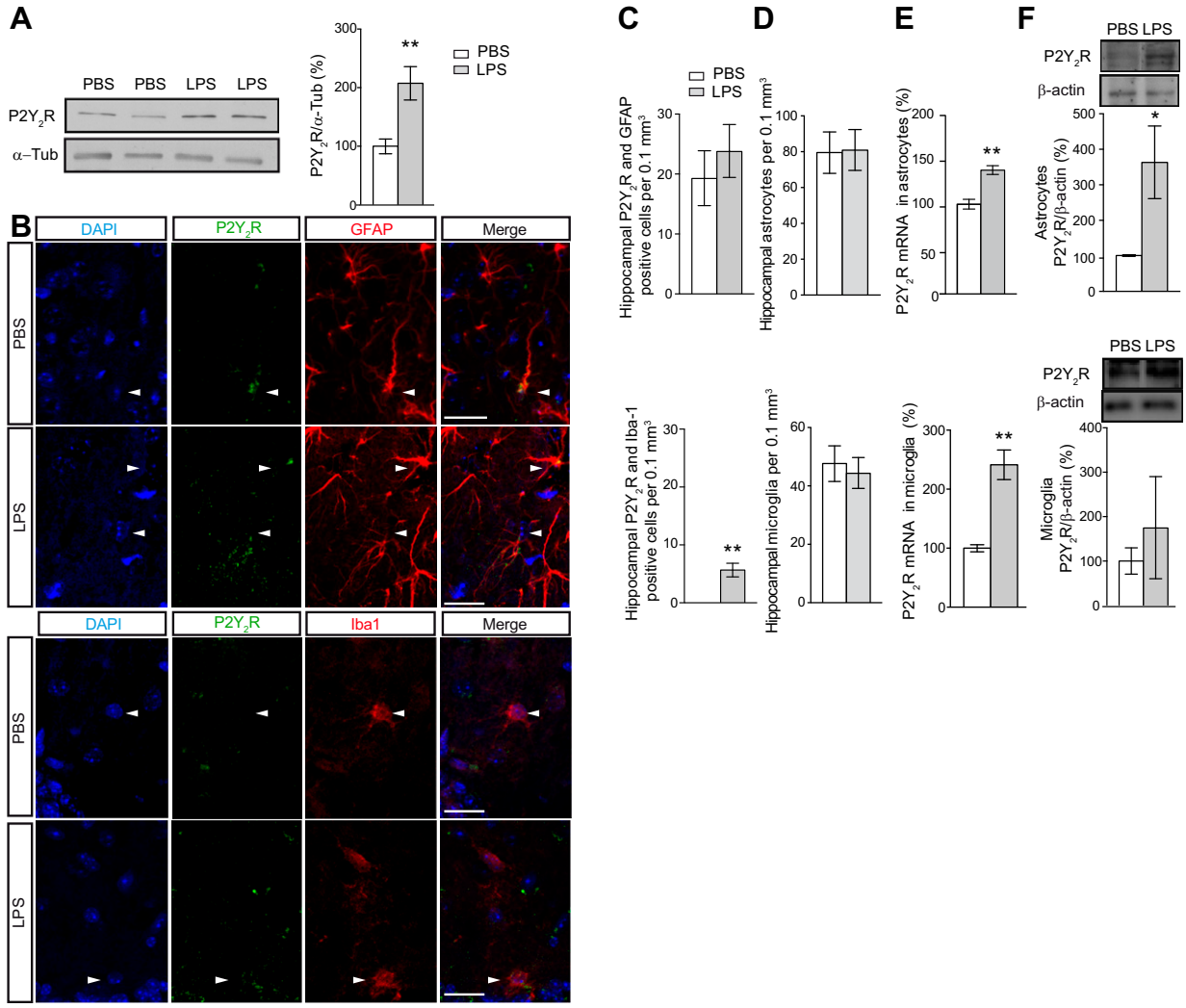

Figure 2. LPS-induced neuroinflammation increases $P2Y_2R$ expression in glial cells. *A*) Western blot analysis of $P2Y_2R$ expression in hippocampal samples from intraperitoneal PBS- or LPS-treated 6-mo-old UbGFP mice. Membranes are probed with an anti-tubulin (a-Tub) antibody to correct for any possible deviation on protein loading. One hundred percent corresponds to $P2Y_2R$ protein expression detected in PBS-treated UbGFP mice ($n \geq 5$ mice/treatment). *B*) Representative micrographs of astrocytes (GFAP positive) and microglial cells (Iba-1 positive) in hippocampal sections from intraperitoneal PBS- or LPS-treated UbGFP mice expressing $P2Y_2R$. The localization of $P2Y_2R$ in GFAP- or Iba-1-positive cells is indicated by arrowheads. Original scale bars, 20 μm. *C*) Quantification of astrocytes and microglial cells expressing $P2Y_2R$/0.1 mm^3 in hippocampal sections from PBS- or LPS-treated UbGFP mice. *D*) Total number of astrocytes and microglia cells/0.1 mm^3 in hippocampal sections from PBS- or LPS-treated UbGFP mice. *E*) Quantification of mRNA and (*F*) protein levels of $P2Y_2R$, both in cultured astrocytes and microglial cells from the hippocampus of WT mice. Cultures were treated with PBS or LPS 0.3 μg/ml for 48 h. Values represent, at least, the means ± SEM of 3 independent cultures run in duplicate. $^*P < 0.05$, $^{**}P < 0.01$ (unpaired Student's *t* test).

interaction. Nevertheless, although the LPS treatment induced a comparable reduction in the body weight of both UbGFP and UbGFP; $P2Y_2R^{-/-}$ mice (Fig. 4*B*), we detect statistically significant differences regarding the social interaction test. Compared with PBS-treated mice, LPS induced a statistically significant reduction of the social

corresponds to the Ub^{G76V}-GFP mRNA levels detected in UbGFP mice treated with PBS intraperitoneally. *D*) Representative micrographs of hippocampal sections from 6-mo-old UbGFP mice treated with PBS or LPS and double-stained with antibodies against GFP protein (green) and the specific astrocytic marker GFAP, the microglial marker Iba-1, or neuronal marker NeuN. Colocalization is indicated by arrowheads. Original scale bars, 20 μm. *E*) Quantification of the number of GCDG positively identified as astrocytes, microglial cells, or neurons per 0.1 mm^3 hippocampal DG in PBS- or LPS-treated UbGFP mice ($n \geq 4$ mice/treatment; sections ≥6/mouse). *F*) Representative images of Western blot using hippocampal samples from 6-mo-old intraperitoneal PBS- or LPS-treated UbGFP mice and stained with antibodies against constitutive (β1, β2, and β5) or inducible (β1i, β2i, and β5i) proteasome catalytic β subunits. Graphs show quantification of the protein expression of proteasome catalytic β subunits ($n \geq 9$ mice/treatment). Membranes are probed with an anti-tubulin (α-Tub) antibody to correct for any possible deviation on protein loading. The value of 100% corresponds to the expression of the corresponding β protein detected in intraperitoneally PBS-treated UbGFP mice. Data in bar graphs depict means ± SEM. $^*P < 0.05$, $^{***}P < 0.001$, $^{****}P < 0.0001$ [unpaired Student's *t* test (*E*, *F*)], $^{**}P < 0.001$, $^{****}P < 0.0001$ [1-way ANOVA, followed by Bonferroni's test (*B*)].

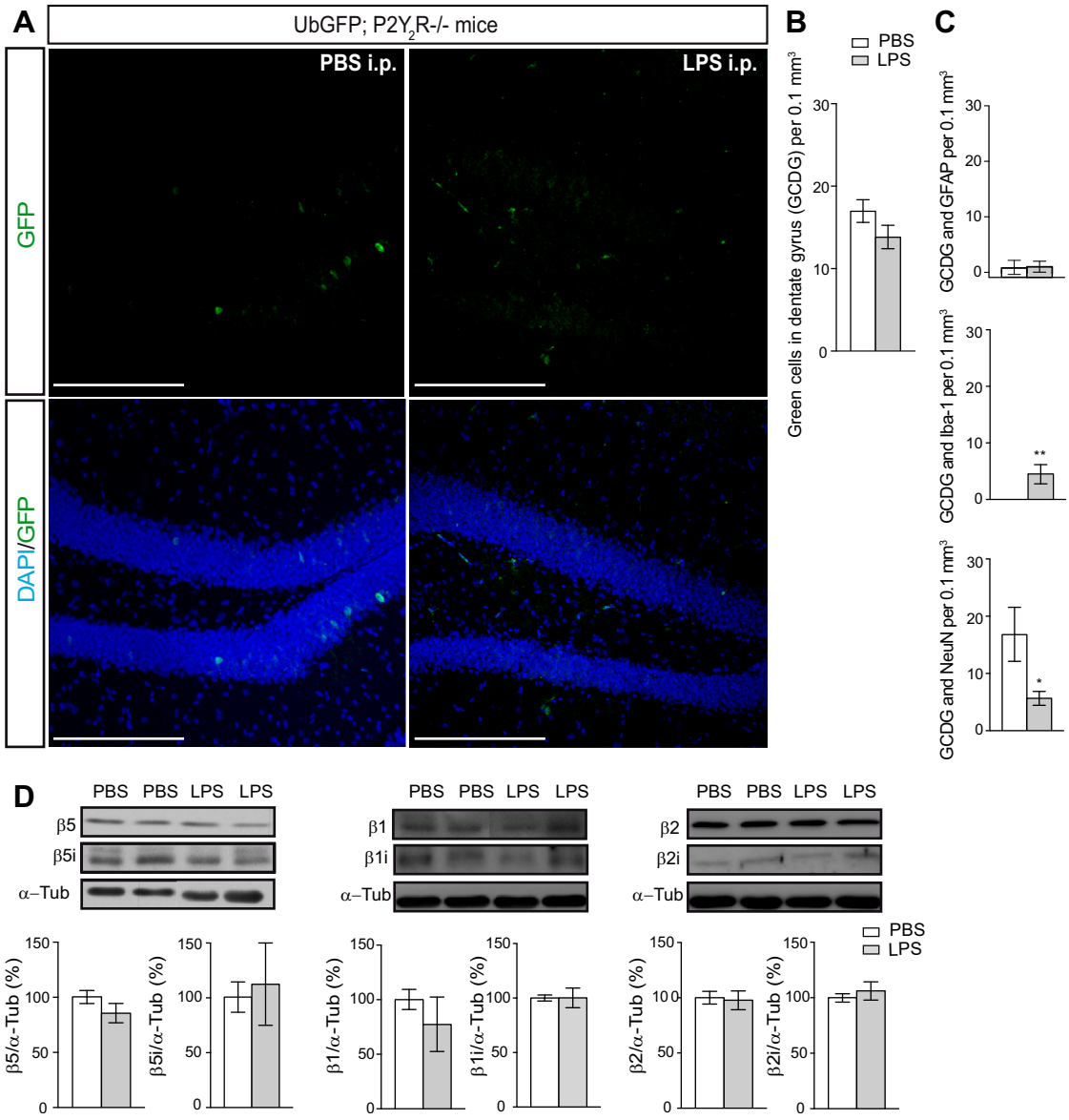

Figure 3. $P2Y_2R^{-/-}$ mice did not show the UPS impairment in astrocytes induced by LPS. *A*) Representative images of hippocampal coronal sections from treated UbGFP; $P2Y_2R^{-/-}$ mice treated with PBS or LPS (intraperitoneal) and stained with an antibody against GFP alone (upper) or with DAPI (lower). Original scale bars, 200 μm. *B*) The graph shows the quantification of GCDG/0.1 mm^3 hippocampal DG ($n \geq 6$ mice/treatment; sections ≥7/mouse). *C*) Quantification of the number of GCDG positively identified as astrocytes, microglial cells, or neurons/0.1 mm^3 hippocampal DG from intraperitoneal PBS- or LPS-treated UbGFP; $P2Y_2R^{-/-}$ mice ($n \geq 4$ mice/genotype and treatment; sections ≥6/mouse). *D*) Representative images of Western blot using hippocampal samples from intraperitoneal PBS- or LPS-treated 6-mo-old UbGFP; $P2Y_2R^{-/-}$ mice with antibodies against constitutive (β1, β2, and β5) or inducible (β1i, β2i, and β5i) proteasome catalytic β subunits. Quantification of the protein expression of proteasome catalytic β subunits ($n \geq 4$ mice/treatment). Membranes are probed with an anti-tubulin antibody to correct for any possible deviation on protein loading. One hundred percent value corresponds to the protein expression of β subunits detected in PBS-treated UbGFP; $P2Y_2R^{-/-}$ mice. Data in bar graphs depict means ± SEM. $^*P < 0.05$, $^{**}P < 0.01$ (unpaired Student's *t* test).

behavior in UbGFP mice at all times tested, whereas the UbGFP; $P2Y_2R^{-/-}$ mice presented similar social interaction at T1′ and T4′ (10 min and 24 h post-LPS injection, respectively; Fig. 4*B*). Hence, the LPS-treated UbGFP; $P2Y_2R^{-/-}$ mice showed a higher social interaction than LPS-treated UbGFP mice, both at T1′ (10 min post-injection; UbGFP 5.1 ± 2.9% *vs.* UbGFP; $P2Y_2R^{-/-}$ 34.1 ± 19.5%) and at T4′ (24 h postinjection; UbGFP 0.0 ± 0.0% *vs.* UbGFP; $P2Y_2R^{-/-}$ 29.3 ± 17.1%; Fig. 4*B*).

As we have demonstrated in a previous study that pharmacological inhibition of $P2Y_2R$ induced a significant accumulation of Ub^{G76V}-GFP in neuroblastoma cells expressing this UPS reporter (24), we wonder whether the Ub^{G76V}-GFP protein accumulation in the LPS-treated UbGFP mice may be a result of the endotoxin affecting $P2Y_2R$ functionality. To address this question, UbGFP mice were intracerebroventricularly treated with 2 μl of 1.5 mM suramin, a $P2Y_2R$ antagonist, after having the

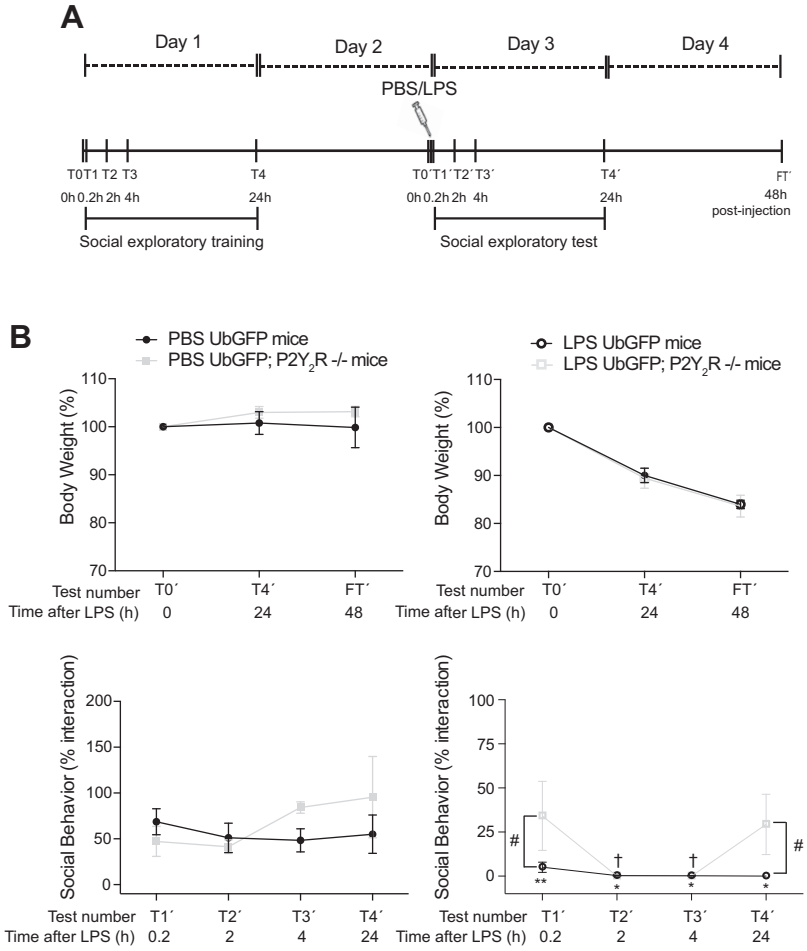

Figure 4. $P2Y_2R$ contributes to altering the social behavior associated with LPS-induced neuroinflammation. *A*) Schematic representation of the followed protocol in social behavior tests. T, test number; FT, final test day. *B*) Graphs represent the evolution of body weight (upper) and the variations on social interaction (lower) of UbGFP mice (black) and UbGFP; $P2Y_2R^{-/-}$ mice (gray) after the PBS (solid circles and squares) or LPS (open circles and squares) administration. One hundred percent value corresponds to the initial body weight of each genotype or the social interaction time at the first day of social exploratory training, respectively. The tests referred to as T1′, T2′, T3′, and T4′ correspond to 10 min and 2, 4, and 24 h after LPS injection, respectively. Data in graphs represent the means ± SEM from $n \geq 7$ mice/genotype and treatment. $^{*}P < 0.05$, $^{**}P < 0.01$ between PBS- and LPS-treated UbGFP mice, $^{\dagger}P < 0.05$ between PBS- and LPS-treated UbGFP; $P2Y_2R^{-/-}$ mice, $^{\#}P < 0.05$ between LPS-treated UbGFP mice and LPS-treated UbGFP; $P2Y_2R^{-/-}$ mice (2-way ANOVA, followed by Sidak's test).

intraperitoneal injection of LPS or PBS. Forty-eight hours after intraperitoneal injection, the animals were euthanized to be analyzed (**Fig. 5*A***). The results showed that suramin caused a similar increase in the number of GCDG (34.6 ± 1.9 GCDG/0.1 mm^3; Fig. 5*B, C*) to that produced by intraperitoneal LPS administration (Fig. 1*A, B*). However, when mice were treated with LPS plus suramin, no additive effect in the total number of GCDG was observed (22.7 ± 3.9 GCDG/0.1 mm^3; Fig. 5*B, C*). In a similar way, no additive effect between either treatment was observed, in the number of green microglia, green astrocytes, or green neuronal cells (Fig. 5*D*). These data suggest that both compounds, suramin and LPS, modulate the activity of the UPS through a common molecular mechanism.

Selective $P2Y_2R$ activation prevents the LPS-induced UPS impairment in astrocytes

Our next step was to evaluate if a selective activation of $P2Y_2R$ may counter the LPS-induced UPS impairment in glial cells. To answer this question, both UbGFP and UbGFP; $P2Y_2R^{-/-}$ mice were treated intracerebroventricularly with 2 μl of 45 mM Up_4U, a selective $P2Y_2R$ agonist, or with the same volume of PBS, 24 h after intraperitoneal injection of LPS or PBS. Forty-eight hours after intraperitoneal injection, animals were euthanized to be analyzed (**Fig. 6*A***). As shown in Fig. 6*B*, UbGFP mice treated with LPS plus Up_4U presented statistically, significantly less GCDG than UbGFP mice treated with LPS plus PBS (LPS + PBS 25.4 ± 2.4 GCDG/0.1 mm^3 *vs.* LPS + Up_4U 18.0 ± 2.2 GCDG/0.1 mm^3). Moreover, no significant differences in the number of GCDG between PBS + PBS-treated and LPS + Up_4U-treated UbGFP mice were observed (Fig. 6*B, C*). Involvement of $P2Y_2R$ on effects mediated by Up_4U was definitively confirmed, observing that Up_4U did not significantly modify the number of GCDG in PBS- or LPS-treated UbGFP; $P2Y_2R^{-/-}$ mice (Fig. 6*B, C*). The lineage distribution analysis confirmed that proteostasis alteration induced by LPS in astrocytes was totally reversed by $P2Y_2R$ activation (Fig. 6*D*). However, the Up_4U administration reduced the number but did not totally abolish the microglial cells that presented an accumulation of Ub^{G76V}-GFP protein (LPS + PBS 9.3 ± 4.3 GCDG/0.1 mm^3 *vs.* LPS + Up_4U 5.0 ± 2.1 GCDG/0.1 mm^3; Fig. 6*D*). Interestingly, when Up_4U was assayed in cultures of hippocampal microglial cells, a significant increase in CT-L proteasomal activity, associated with an increased expression of the β5 subunit, was detected (Supplemental Fig. 2*A, B*). However, as in UbGFP; $P2Y_2R^{-/-}$ mice, some microglial cells still showed a significant accumulation of the UPS reporter, we cannot rule out that other factors, besides $P2Y_2R$, are involved in the UPS alteration induced by LPS in this lineage.

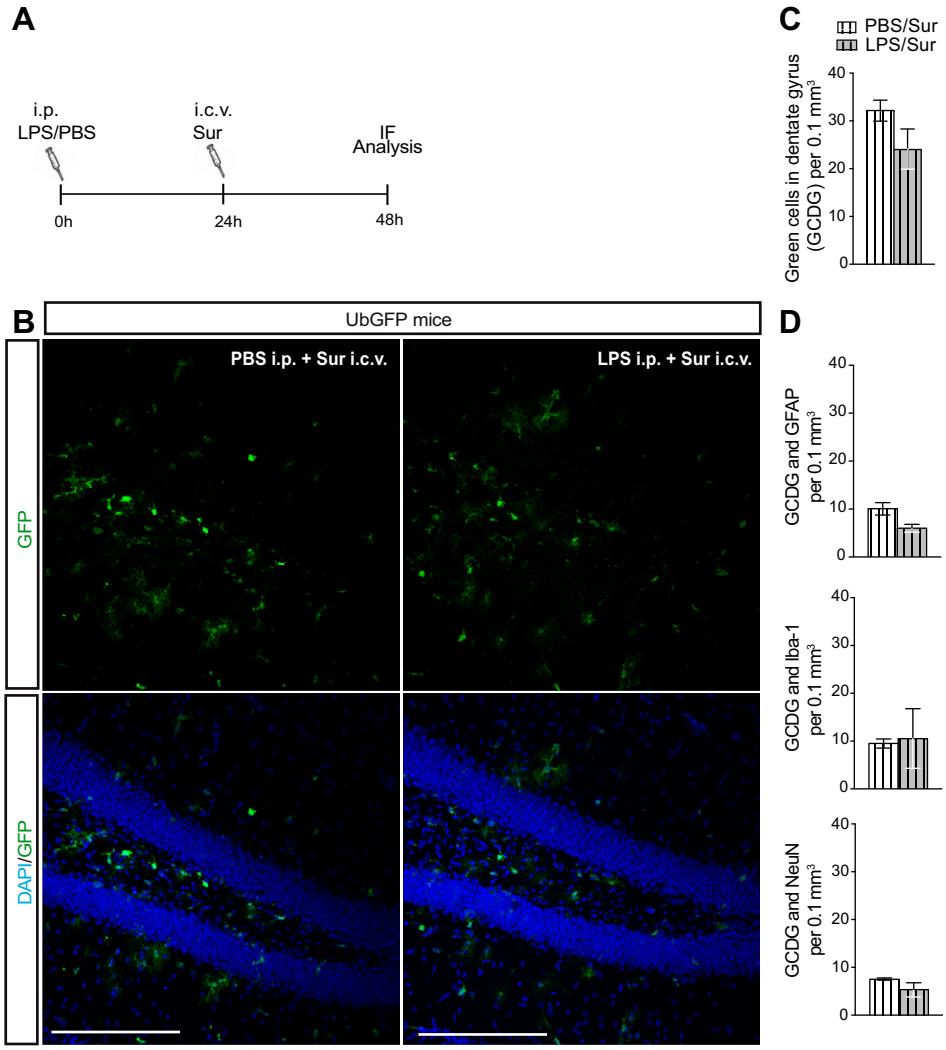

Figure 5. Suramin (Sur) and LPS did not produce additive effects on glial proteostasis. *A*) Schematic representation of the followed protocol. IF, immunofluorescence. *B*) Representative images of hippocampal coronal sections from UbGFP mice treated with PBS + suramin or LPS + suramin and stained with antibody against GFP alone (upper) or with the nuclear marker DAPI (lower). Original scale bars, 200 μm. *C*) The graph shows the quantification of GCDG/0.1 mm^3 hippocampal tissue from UbGFP mice treated intraperitoneally with PBS and intracerebroventricularly with suramin (white-striped bar) or intraperitoneally with LPS and intracerebroventricularly with suramin (gray-striped bar; $n \geq 4$ mice/treatment; sections ≥5/mouse). *D*) Quantification of GCDG positively identified as astrocytes, microglial cells, or neurons/0.1 mm^3 hippocampal DG in UbGFP mice treated as indicated in *C* ($n \geq 4$ mice/genotype and treatment; sections ≥6/mouse). Statistical significance was not detected using unpaired Student's *t* test. Data in bar graphs depict means ± SEM.

Expression levels of β5 and β5i subunits were also analyzed in UbGFP and UbGFP; $P2Y_2R^{-/-}$ mice, treated or not with LPS in the presence or absence of Up_4U (Fig. 6*E*). Results revealed that the reduction of β5 expression, induced by LPS, was not observed in UbGFP mice treated with LPS plus Up_4U (Fig. 6*E*). In a similar way, the increased expression of the β5i subunit, detected in LPS-treated mice, was not observed in LPS + Up_4U-treated UbGFP mice (Fig. 6*E*). Independently of the treatment applied, no significant modification in the levels of β5 or β5i was detected in UbGFP; $P2Y_2R^{-/-}$ mice (Fig. 6*E*).

To validate fully the involvement of $P2Y_2R$ in the alteration of UPS in astrocytes induced by LPS and to identify the underlying intracellular pathway, we performed additional studies using hippocampal astrocyte cultures from WT and $P2Y_2R^{-/-}$ mice and the human glioblastoma astrocytoma cell line U87. These studies confirmed that the UPS inhibition induced by LPS was dose dependent (Supplemental Fig. 1*C*) and that stimulation of astrocytes from WT mice with 100 μM Up_4U for 24 h increased their proteasomal CT-L, as it induces the expression of the proteasomal catalytic β5 subunit on them by a mechanism dependent on both the nonreceptor tyrosine kinases family (Src) and PI3K (**Fig. 7*A*, *B***). Moreover and in line with *in vivo* studies, the cotreatment of astrocytes with 0.3 μg/ml LPS plus 100 μM Up_4U avoided the decrease in CT-L activity caused by LPS 0.3 μg/ml (Fig. 7*C*). Up_4U did not induce changes on CT-L activity in cultured astrocytes from $P2Y_2R^{-/-}$ mice, confirming the involvement of $P2Y_2R$ (Fig. 7*C*). It is also worth highlighting that Up_4U-induced $P2Y_2R$ activation significantly countered the inhibition of proteasomal CT-L activity but not the PG-L activity induced by the selective and irreversible proteasome inhibitor, epoxomicin (Fig. 7*D*).

DISCUSSION

It has been proposed that a neuroinflammatory status leads to an imbalance of cellular proteostasis by altering the proteasome activity (8). Thereby, the cytokines or LPS-induced neuroinflammation promote the proteasomal-dependent production of proinflammatory mediators in microglial cells (12) or cause an increase of proteasomal CT-L activity in astrocytes (31). Based on these studies, selective proteasomal inhibitors, such as epoxomicin, have been postulated as potent anti-inflammatory agents (32). However, other groups have provided evidence indicating

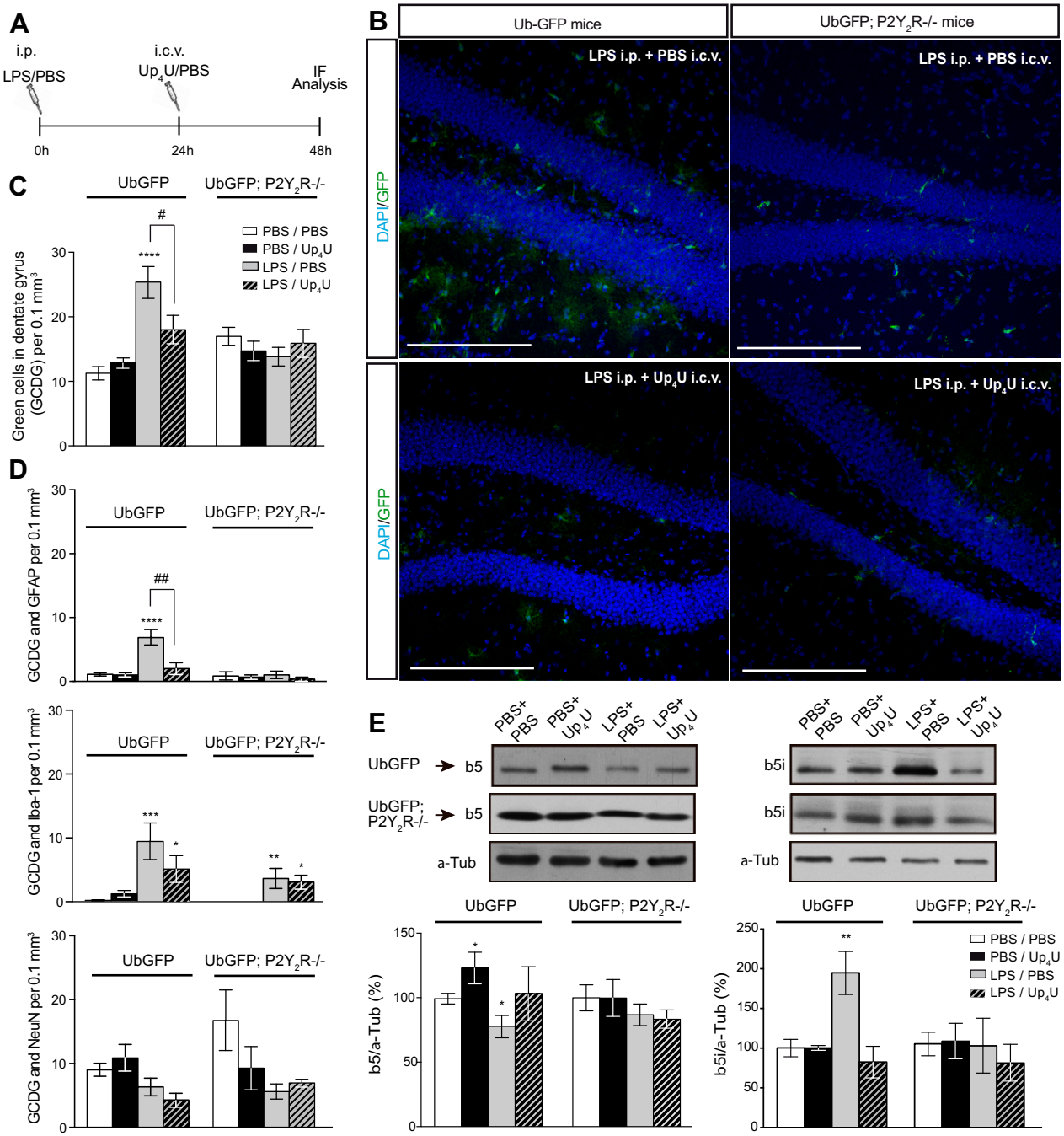

Figure 6. Intracerebroventricula administration of Up_4U reverted the UPS impairment induced by LPS in astrocytes. *A*) Schematic representation of the followed protocol. *B*) Representative images of hippocampal coronal sections from UbGFP and UbGFP; $P2Y_2R^{-/-}$ mice treated with LPS or LPS + Up_4U and stained with an antibody against GFP plus DAPI. Original scale bars, 200 μm. *C*) Quantification of GCDG/0.1 mm^3 hippocampal tissue from UbGFP and UbGFP; $P2Y_2R^{-/-}$ mice treated as follows: intraperitoneally and intracerebroventricularly with PBS (white bar), intraperitoneally with PBS and intracerebroventricularly with Up_4U (black bar), intraperitoneally with LPS and intracerebroventricularly with PBS (gray bar) or intraperitoneally with LPS and intracerebroventricularly with Up_4U (gray-striped bar; $n \geq 4$ mice/treatment; sections ≥7/mouse). *D*) Quantification of GCDG positively identified as astrocytes, microglial cells, or neurons/0.1 mm^3 hippocampal DG in UbGFP and UbGFP; $P2Y_2R^{-/-}$ mice treated as indicated in *C* ($n \geq 4$ mice/genotype and treatment; sections ≥5/mouse). *E*) Representative images of Western blot using hippocampal samples from 6-mo-old UbGFP and UbGFP; $P2Y_2R^{-/-}$ mice treated as indicated in *C* with antibodies against β5 or β5i proteasome catalytic subunits. Graphs show quantification of the protein expression of proteasome catalytic β5 or β5i subunits ($n \geq 4$ mice/genotype and treatment). Membranes are probed with an anti-tubulin antibody to correct for any possible deviation on protein loading. One hundred percent value corresponds to the protein expression of β5 or β5i detected in PBS-treated UbGFP or UbGFP; $P2Y_2R^{-/-}$ mice. Data in bar graphs depict means ± SEM. $^*P < 0.05$, $^{**}P < 0.01$, $^{***}P < 0.001$, $^{****}P < 0.0001$ [1-way ANOVA, followed by Bonferroni's test when compared with PBS/PBS (*C–E*)] $^{\#}P < 0.05$, $^{\#\#}P < 0.01$ [1-way ANOVA, followed by Bonferroni's test when compared with LPS/Up_4U (*C, D*)].

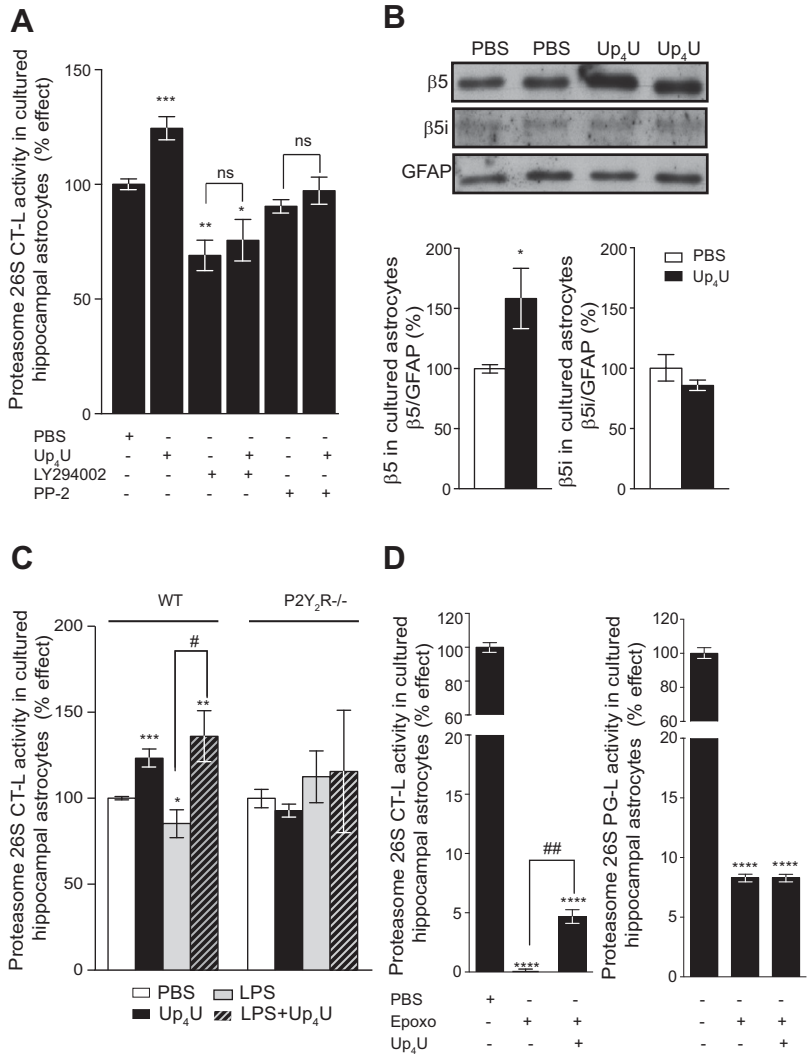

Figure 7. $P2Y_2R$ activation reverted the LPS-induced UPS impairment in astrocytes increasing CT-L activity *via* inducing the proteasome subunit β5 expression in a mechanism involving Src/MEK. *A*) Proteasomal CT-L activity measured in hippocampal astrocyte cultures from UbGFP mice treated for 24 h with 100 μM Up_4U. Astrocytes were pretreated or not with LY294002 (50 μM), a selective inhibitor of PI3K, or PP-2 (2 μM), a selective inhibitor of the Src tyrosine kinase, for 20 min before adding the dinucleotide to the culture medium. One hundred percent value corresponds to the CT-L activity measured in hippocampal astrocytes treated with PBS ($n \geq 4$ independent cultures run in triplicate). *B*) Representative images of Western blot from astrocytes treated with PBS or 100 μM Up_4U for 24 h with antibodies against β5 or β5i proteasome catalytic subunits. Graphs show quantification of the protein expression of proteasome catalytic β5 or β5i subunits ($n \geq 4$ independent cultures run in duplicate). Membranes are probed with an anti-GFAP antibody to correct for any possible deviation on protein loading. One hundred percent value corresponds to the protein expression of β5 or β5i detected in cultures treated with PBS. *C*) Proteasomal CT-L activity measured in hippocampal astrocytes cultured from WT mice and $P2Y_2R^{-/-}$ mice. One hundred percent value corresponds to the CT-L activity measured in cultured hippocampal astrocytes from WT and $P2Y_2R^{-/-}$ mice treated with PBS, respectively ($n \geq 4$ independent cultures run in quadruplicate). *D*) The graphs show the proteasomal CT-L and PG-L activities measured in cultured hippocampal astrocytes, pretreated or not with epoxomicin (Epoxo) 5 μM for 20 min and 100 μM Up_4U for 24 h. One hundred percent value corresponds to the CT-L or PG-L activities measured in hippocampal astrocytes treated with PBS ($n \geq 4$ independent cultures run in quadruplicate). Data in bar graphs depict means ± SEM. $^*P < 0.05$ [unpaired Student's *t* test. (*B*)], $^*P < 0.05$, $^{**}P < 0.01$, $^{***}P < 0.001$, $^{****}P < 0.0001$ [1-way ANOVA, followed by Bonferroni's test when compared with PBS (*A, C, D*)], $^{\#}P < 0.05$, $^{\#\#}P < 0.01$ [unpaired Student's *t* test (*A*)].

that the LPS-induced neuroinflammation causes UPS impairment, and thereby, proteasome inhibitors would not only revert but would actually potentiate the LPS-induced neuroinflammation (10, 11). In the present work, with the use of a UPS reporter mouse model (UbGFP mice), we provide new evidences indicating that LPS-induced acute neuroinflammation compromises the cellular proteolysis in both astroglial and microglial cells by a mechanism involving $P2Y_2R$. Supporting this hypothesis, LPS-treated UbGFP mice lacking $P2Y_2R$ did not present a significant UPS impairment in astrocytes nor a social interaction deficit as severe as that observed in LPS-treated UbGFP mice. Moreover, the *in vivo* administration of Up_4U, a selective $P2Y_2R$ agonist, reverted the UPS impairment in astrocytes caused by an LPS-induced neuroinflammation. Our studies also revealed that the Up_4U-induced $P2Y_2R$ activation leads to the activation of Src/PI3K/ERK1/2. Mobilization of this intracellular signaling pathway increases the expression of the proteasomal β5 subunit, offsetting the reduction of this caused by LPS and preventing its replacement by the β5i subunit.

LPS administration causes neuroinflammation status through TLR4 activation (9). The molecular pathways involved, including activation of proinflammatory transcription factors, such as NF-κB, synthesis, and processing, and release of proinflammatory mediators, as well as ATP release (18, 33). As NF-κB upregulates the $P2Y_2R$ transcription under proinflammatory conditions (34), it was postulated that $P2Y_2R$ plays a relevant role in LPS-induced neuroinflammation. Indeed, the increased expression of functional $P2Y_2R$ under inflammatory status allows the alveolar cells to increase their secretory rate (33), potentiates the LPS-induced neutrophil transendothelial migration (20), enhances the migration and phagocytosis ability of microglial cells during postnatal brain development (21), and facilitates the secretion of proinflammatory mediators induced by LPS (18). In line with the studies suggesting that $P2Y_2R$ plays a proinflammatory role, our results suggest that LPS induced a proteolysis impairment in glial cells in WT mice but not in $P2Y_2R^{-/-}$ mice. Nevertheless, it should be noted that Up_4U-treated mice did not show a UPS impairment, but they present an increase

in CT-L activity and the concomitant upregulation of proteasomal β5 subunits, as previously reported (24). Because we have demonstrated that LPS-induced acute neuroinflammation compromises the cellular proteolysis in astroglial cells, it seems reasonable to think that $P2Y_2R$ activation in astrocytes would not contribute to the promotion of a proinflammatory status.

Conversely, the anti-inflammatory role of $P2Y_2R$ has also been suggested. Thus, it has been reported that nucleotides attenuate the LPS-induced production of cytokines and NO in macrophages (23), reduced the release of TNF-α, IL-6, and NO in microglial cells (22), and downregulated the gene expression of CD14 myeloid differentiation primary response 88, caused by LPS-induced TLR4 activation (35). In addition, as ATP and UTP downregulated the gene expression of TLR4 and the phosphorylation of NF-κB induced by TLR4 activation, it was postulated that $P2Y_2Rs$ can negatively regulate TLR4 (35), although the underlying molecular mechanism remains poorly understood. In line with the existence of a close relationship between $P2Y_2R$ and TLR4, we observed that the *in vivo* administration of Up_4U avoided the UPS impairment induced by the endotoxin in glial cells. Furthermore, we found that the decrease of cellular proteolysis in glial cells, induced by inhibiting $P2Y_2R$ or by activating TLR4 by LPS, is not an additive process, suggesting that both receptors share a common molecular mechanism. Based on our previous work, reporting that the blocking of $P2Y_2R$ induces a UPS impairment (24), we can reason that endotoxin alters the astrocytic proteolysis by inducing a heterologous desensitization of $P2Y_2R$. This hypothesis is based on TLR4 activation triggers, among others, PKC activation (36), which would induce phosphorylation of the C-terminal tail of $P2Y_2Rs$, causing the heterologous desensitization of them (37). In line with this hypothesis, we can reason that the lack of effect of LPS on $P2Y_2R^{-/-}$ mice may be a result of LPS altering the astrocytic proteolysis by blocking the tonic activity of $P2Y_2R$. Moreover, as Src, an essential kinase for the proinflammatory response induced by TLR4 activation in astrocytes (38), has been involved in the formation of the protein complex between epithelial growth factor receptor and $P2Y_2R$ (39), it is reasonable to think that a similar protein complex can be formed between TLR4 and $P2Y_2R$, which would favor a fine crossregulation between both receptors. On the other hand, as the TLR4 activation by LPS also promotes the transcription of $P2Y_2R$ (18), we postulate that *de novo* synthesis of β5 subunits induced by activation of new $P2Y_2R$ (24) may be the mechanism by which Up_4U reverts the UPS impairment induced by LPS. Although we recommend additional studies to confirm this hypothesis, the studies carried out in astrocyte cultures showed that the inhibition of CT-L activity by epoxomicin was significantly countered by Up_4U-induced $P2Y_2R$ activation. As the epoxomicin is an irreversible proteasome inhibitor, it reasonable to think that the effect induced by Up_4U requires the synthesis of new β5 subunits, as we have previously reported (24).

In the present study, we have demonstrated that the inhibition of $P2Y_2R$ by LPS is essential for this toxin to induce an acute neuroinflammatory status. As a result of this blockage, a proteasomal proteolysis impairment, especially in astrocytes, is induced, which leads them to alter their cellular proteostasis, favoring, in this way, the reactive astrocytosis. Our results also suggest that the selective $P2Y_2R$ agonist, Up_4U, a compound already commercialized as diquafosol in Japan and South Korea for the treatment of dry eye (40), might have anti-inflammatory properties, as it is able to return the proteostasis balance to astrocytes. FJ

ACKNOWLEDGMENTS

This work was supported by funding from the Spanish Ministry of Science and Education (BFU2012-31195; European Union Project H2020-MSCA-ITN-2017, No. 766124 to M.D.-H.) and Universidad Complutense of Madrid (UCM)–Santander Central Hispano Bank (911585-670 to M.D.-H.). A.S.-S. was funded by Grant BFU2012-31195; L.D.D.-G. has a UCM predoctoral fellowship supervised by M.D.-H, and J.J.L. received Fundación Banco Bilbao Vizcaya Argentaria (BBVA) grants from CiberNed–ISCIII PI2015-2/06-3 (Collaborative), and from Mineco SAF2015-65371-R. The authors declare no conflicts of interest.

AUTHOR CONTRIBUTIONS

L. de Diego-García and M. Díaz-Hernández designed research; L. de Diego-García, Á. Sebastián-Serrano, and M. Díaz-Hernández analyzed the data; L. de Diego-García and I. H. Hernández performed the research; M. Díaz-Hernández wrote the paper; J. Pintor and J. J. Lucas contributed new reagents; and L. de Diego-García, Á. Sebastián-Serrano, J. Pintor, and J. J. Lucas revised the manuscript.

REFERENCES

1. Martinon, F., and Aksentijevich, I. (2015) New players driving inflammation in monogenic autoinflammatory diseases. *Nat. Rev. Rheumatol.* **11**, 11–20
2. Brehm, A., and Krüger, E. (2015) Dysfunction in protein clearance by the proteasome: impact on autoinflammatory diseases. *Semin. Immunopathol.* **37**, 323–333
3. Shin, J. N., Fattah, E. A., Bhattacharya, A., Ko, S., and Eissa, N. T. (2013) Inflammasome activation by altered proteostasis. *J. Biol. Chem.* **288**, 35886–35895
4. Kaushik, S., and Cuervo, A. M. (2015) Proteostasis and aging. *Nat. Med.* **21**, 1406–1415
5. Hershko, A., and Ciechanover, A. (1998) The ubiquitin system. *Annu. Rev. Biochem.* **67**, 425–479
6. Schwartz, A. L., and Ciechanover, A. (2009) Targeting proteins for destruction by the ubiquitin system: implications for human pathobiology. *Annu. Rev. Pharmacol. Toxicol.* **49**, 73–96
7. Pickart, C. M., and Cohen, R. E. (2004) Proteasomes and their kin: proteases in the machine age. *Nat. Rev. Mol. Cell Biol.* **5**, 177–187
8. Glickman, M. H., and Raveh, D. (2005) Proteasome plasticity. *FEBS Lett.* **579**, 3214–3223
9. Pla, A., Pascual, M., Renau-Piqueras, J., and Guerri, C. (2014) TLR4 mediates the impairment of ubiquitin-proteasome and autophagy-lysosome pathways induced by ethanol treatment in brain. *Cell Death Dis.* **5**, e1066
10. Jamart, C., Gomes, A. V., Dewey, S., Deldicque, L., Raymackers, J. M., and Francaux, M. (2014) Regulation of ubiquitin-proteasome and autophagy pathways after acute LPS and epoxomicin administration in mice. *BMC Musculoskelet. Disord.* **15**, 166
11. Pintado, C., Gavilán, M. P., Gavilán, E., García-Cuervo, L., Gutiérrez, A., Vitorica, J., Castaño, A., Ríos, R. M., and Ruano, D. (2012) Lipopolysaccharide-induced neuroinflammation leads to the

accumulation of ubiquitinated proteins and increases susceptibility to neurodegeneration induced by proteasome inhibition in rat hippocampus. *J. Neuroinflammation* **9**, 87
12. Bi, W., Zhu, L., Zeng, Z., Jing, X., Liang, Y., Guo, L., Shi, Q., Xu, A., and Tao, E. (2014) Investigations into the role of 26S proteasome non-ATPase regulatory subunit 13 in neuroinflammation. *Neuroimmunomodulation* **21**, 331–337
13. Shi, J., Liu, X., Xu, C., Ge, J., Ren, J., Wang, J., Song, X., Dai, S., Tao, W., and Lu, H. (2015) Up-regulation of PSMB4 is associated with neuronal apoptosis after neuroinflammation induced by lipopolysaccharide. *J. Mol. Histol.* **46**, 457–466
14. Burnstock, G. (2007) Physiology and pathophysiology of purinergic neurotransmission. *Physiol. Rev.* **87**, 659–797
15. Shen, J., Seye, C. I., Wang, M., Weisman, G. A., Wilden, P. A., and Sturek, M. (2004) Cloning, up-regulation, and mitogenic role of porcine P2Y2 receptor in coronary artery smooth muscle cells. *Mol. Pharmacol.* **66**, 1265–1274
16. Schrader, A. M., Camden, J. M., and Weisman, G. A. (2005) P2Y2 nucleotide receptor up-regulation in submandibular gland cells from the NOD.B10 mouse model of Sjögren's syndrome. *Arch. Oral Biol.* **50**, 533–540
17. Rodríguez-Zayas, A. E., Torrado, A. I., and Miranda, J. D. (2010) P2Y2 receptor expression is altered in rats after spinal cord injury. *Int. J. Dev. Neurosci.* **28**, 413–421
18. Eun, S. Y., Seo, J., Park, S. W., Lee, J. H., Chang, K. C., and Kim, H. J. (2014) LPS potentiates nucleotide-induced inflammatory gene expression in macrophages via the upregulation of P2Y2 receptor. *Int. Immunopharmacol.* **18**, 270–276
19. Weisman, G. A., Camden, J. M., Peterson, T. S., Ajit, D., Woods, L. T., and Erb, L. (2012) P2 receptors for extracellular nucleotides in the central nervous system: role of P2X7 and $P2Y_2$ receptor interactions in neuroinflammation. *Mol. Neurobiol.* **46**, 96–113
20. Kukulski, F., Ben Yebdri, F., Bahrami, F., Fausther, M., Tremblay, A., and Sévigny, J. (2010) Endothelial P2Y2 receptor regulates LPS-induced neutrophil transendothelial migration in vitro. *Mol. Immunol.* **47**, 991–999
21. Sunkaria, A., Bhardwaj, S., Halder, A., Yadav, A., and Sandhir, R. (2016) Migration and phagocytic ability of activated microglia during post-natal development is mediated by calcium-dependent purinergic signalling. *Mol. Neurobiol.* **53**, 944–954
22. Boucsein, C., Zacharias, R., Färber, K., Pavlovic, S., Hanisch, U. K., and Kettenmann, H. (2003) Purinergic receptors on microglial cells: functional expression in acute brain slices and modulation of microglial activation in vitro. *Eur. J. Neurosci.* **17**, 2267–2276
23. Guerra, A. N., Fisette, P. L., Pfeiffer, Z. A., Quinchia-Rios, B. H., Prabhu, U., Aga, M., Denlinger, L. C., Guadarrama, A. G., Abozeid, S., Sommer, J. A., Proctor, R. A., and Bertics, P. J. (2003) Purinergic receptor regulation of LPS-induced signaling and pathophysiology. *J. Endotoxin Res.* **9**, 256–263
24. De Diego-García, L., Ramírez-Escudero, M., Sebastián-Serrano, Á., Diaz-Hernández, J. I., Pintor, J., Lucas, J. J., and Díaz-Hernández, M. (2017) Regulation of proteasome activity by P2Y2 receptor underlies the neuroprotective effects of extracellular nucleotides. *Biochim. Biophys. Acta* **1863**, 43–51
25. Lindsten, K., Menéndez-Benito, V., Masucci, M. G., and Dantuma, N. P. (2003) A transgenic mouse model of the ubiquitin/proteasome system. *Nat. Biotechnol.* **21**, 897–902
26. Homolya, L., Watt, W. C., Lazarowski, E. R., Koller, B. H., and Boucher, R. C. (1999) Nucleotide-regulated calcium signaling in lung fibroblasts and epithelial cells from normal and P2Y(2) receptor (-/-) mice. *J. Biol. Chem.* **274**, 26454–26460
27. Díaz-Hernández, M., Valera, A. G., Morán, M. A., Gómez-Ramos, P., Alvarez-Castelao, B., Castaño, J. G., Hernández, F., and Lucas, J. J. (2006) Inhibition of 26S proteasome activity by huntingtin filaments but not inclusion bodies isolated from mouse and human brain. *J. Neurochem.* **98**, 1585–1596
28. Henry, C. J., Huang, Y., Wynne, A., Hanke, M., Himler, J., Bailey, M. T., Sheridan, J. F., and Godbout, J. P. (2008) Minocycline attenuates lipopolysaccharide (LPS)-induced neuroinflammation, sickness behavior, and anhedonia. *J. Neuroinflammation* **5**, 15
29. Godbout, J. P., Chen, J., Abraham, J., Richwine, A. F., Berg, B. M., Kelley, K. W., and Johnson, R. W. (2005) Exaggerated neuroinflammation and sickness behavior in aged mice following activation of the peripheral innate immune system. *FASEB J.* **19**, 1329–1331
30. Kong, Q., Peterson, T. S., Baker, O., Stanley, E., Camden, J., Seye, C. I., Erb, L., Simonyi, A., Wood, W. G., Sun, G. Y., and Weisman, G. A. (2009) Interleukin-1beta enhances nucleotide-induced and alpha-secretase-dependent amyloid precursor protein processing in rat primary cortical neurons via up-regulation of the P2Y(2) receptor. *J. Neurochem.* **109**, 1300–1310
31. Zhang, F. F., Morioka, N., Kitamura, T., Hisaoka-Nakashima, K., and Nakata, Y. (2015) Proinflammatory cytokines downregulate connexin 43-gap junctions via the ubiquitin-proteasome system in rat spinal astrocytes. *Biochem. Biophys. Res. Commun.* **464**, 1202–1208
32. Meng, L., Mohan, R., Kwok, B. H., Elofsson, M., Sin, N., and Crews, C. M. (1999) Epoxomicin, a potent and selective proteasome inhibitor, exhibits in vivo antiinflammatory activity. *Proc. Natl. Acad. Sci. USA* **96**, 10403–10408
33. Garcia-Verdugo, I., Ravasio, A., de Paco, E. G., Synguelakis, M., Ivanova, N., Kanellopoulos, J., and Haller, T. (2008) Long-term exposure to LPS enhances the rate of stimulated exocytosis and surfactant secretion in alveolar type II cells and upregulates P2Y2 receptor expression. *Am. J. Physiol. Lung Cell. Mol. Physiol.* **295**, L708–L717
34. Degagné, E., Grbic, D. M., Dupuis, A. A., Lavoie, E. G., Langlois, C., Jain, N., Weisman, G. A., Sévigny, J., and Gendron, F. P. (2009) P2Y2 receptor transcription is increased by NF-kappa B and stimulates cyclooxygenase-2 expression and PGE2 released by intestinal epithelial cells. *J. Immunol.* **183**, 4521–4529
35. Xiao, Z., Yang, M., Fang, L., Lv, Q., He, Q., Deng, M., Liu, X., Chen, X., Chen, M., Xie, X., and Hu, J. (2012) Extracellular nucleotide inhibits cell proliferation and negatively regulates Toll-like receptor 4 signalling in human progenitor endothelial cells. *Cell Biol. Int.* **36**, 625–633
36. Asehnoune, K., Strassheim, D., Mitra, S., Yeol Kim, J., and Abraham, E. (2005) Involvement of PKCalpha/beta in TLR4 and TLR2 dependent activation of NF-kappaB. *Cell. Signal.* **17**, 385–394
37. González, F. A., Weisman, G. A., Erb, L., Seye, C. I., Sun, G. Y., Velázquez, B., Hernández-Pérez, M., and Chorna, N. E. (2005) Mechanisms for inhibition of P2 receptors signaling in neural cells. *Mol. Neurobiol.* **31**, 65–79
38. Floreani, N. A., Rump, T. J., Abdul Muneer, P. M., Alikunju, S., Morsey, B. M., Brodie, M. R., Persidsky, Y., and Haorah, J. (2010) Alcohol-induced interactive phosphorylation of Src and toll-like receptor regulates the secretion of inflammatory mediators by human astrocytes. *J. Neuroimmune Pharmacol.* **5**, 533–545
39. Liu, J., Liao, Z., Camden, J., Griffin, K. D., Garrad, R. C., Santiago-Pérez, L. I., González, F. A., Seye, C. I., Weisman, G. A., and Erb, L. (2004) Src homology 3 binding sites in the P2Y2 nucleotide receptor interact with Src and regulate activities of Src, proline-rich tyrosine kinase 2, and growth factor receptors. *J. Biol. Chem.* **279**, 8212–8218
40. Nichols, K. K., Yerxa, B., and Kellerman, D. J. (2004) Diquafosol tetrasodium: a novel dry eye therapy. *Expert Opin. Investig. Drugs* **13**, 47–54

Received for publication September 29, 2017.
Accepted for publication December 26, 2017.